

# Force-field dependence of the conformational properties of $\alpha,\omega$ -dimethoxypolyethylene glycol

Version: February 5, 2009

Moritz Winger<sup>1</sup>, Alex H. de Vries<sup>2</sup>, and Wilfred F. van Gunsteren<sup>3</sup>

<sup>1</sup> Laboratory of Physical Chemistry, Swiss Federal Institute of Technology, ETH,  
8093 Zürich, Switzerland

<sup>2</sup> Groningen Biomolecular Sciences and Biotechnology Institute, Department of Bio-  
physical Chemistry, University of Groningen, Nijenborgh 4, 9747 AG Groningen, The  
Netherlands

<sup>3</sup> Corresponding author:

E-mail: [wfvgn@igc.phys.chem.ethz.ch](mailto:wfvgn@igc.phys.chem.ethz.ch), [igc-sec@igc.phys.chem.ethz.ch](mailto:igc-sec@igc.phys.chem.ethz.ch)

Tel: 0041-44-632 5501

Fax: 0041-44-632 1039

## ABSTRACT:

A molecular dynamics (MD) study of  $\alpha,\omega$ -dimethoxypolyethylene glycol has been carried out under various conditions with respect to solvent composition, ionic strength, chain length, force field and temperature. A previous MD study on a 15-mer of polyethyleneglycol (PEG) suggested a helical equilibrium structure that was stabilized by hydrogen bonding and bridging water molecules. Experiments show that PEG is highly soluble in water, and indicate that clustering is not favoured. In the present study using different force fields, the GROMOS force fields 45A3 and 53A6, a variation on the latter 53A6\_OE, and a force field by Smith *et al.* produced different results. For the GROMOS force fields 45A3 and 53A6 no helical structure was found, but formation of more or less compact random coils in aqueous solution due to hydrophobic interactions was observed. For the other two force fields used,  $\alpha,\omega$ -dimethoxypolyethylene glycol stayed flexible and more or less elongated in aqueous solution, more in agreement with experimental observations and the previous MD study.

## KEYWORDS:

molecular dynamics, polyethylene glycol, force field, solvent, ions

# 1 Introduction

Polyethylene glycol or polyethylene oxide (PEG, PEO) is regarded as one of the most important polyethers [1–6]. It shows interesting behaviour in both solid and liquid state [7–9]. PEG is extremely well soluble in water [10, 11]. It is also soluble in methanol, benzene, dichloromethane, but is insoluble in diethyl ether and hexane. It can be coupled to hydrophobic molecules to produce non-ionic surfactants. According to experimental data, PEG dissolves not only in water but also in numerous organic solvents [12]. Nuclear magnetic resonance and other spectroscopic measurements [13–17] show that PEG undergoes significant conformational change when going from water to organic solvents. Light scattering experiments on high molecular weight PEG, for instance, show that PEG has a more extended structure in water than in methanol [10, 11]. When moving two surfaces with long PEG chains attached to them closer together, repulsive interactions between the individual PEG chains could be observed in experimental studies [18, 19]. These experimental observations call for an investigation of the conformational properties of PEG. A molecular-dynamics (MD) computer simulation study of PEG [20] suggests that the polymer forms a helical structure in aqueous solution after 2 ns of simulation. The authors found the helix to be stabilized by a network of hydrogen bonds formed between solute-oxygen atoms and water molecules and between water molecules themselves. More recently,

MD simulations of PEG-water solutions of 12 [21] and 54 [22] ether repeat units for a range of compositions (1-32 polymer chains with 1152-100 water molecules) and temperatures (298-410 K) were reported. The trajectories were compared to neutron scattering data [22] and analysed in terms of hydration structure [21] and dynamics [22]. Another issue is the preference of PEG molecules to spatially cluster in particular solvents. For low-molecular-weight PEG molecules spatial clustering observations are still controversially documented in the literature. Some authors claim that clustering of PEG molecules is caused by impurities [23], whereas other authors think a chain-end effect is responsible for the clustering of PEG [24].

In the molecular dynamics study presented below, the compaction and aggregation properties of  $\alpha,\omega$ -dimethoxypolyethylene glycol (PEG) have been investigated as function of solute composition, chain length, solvent composition, temperature, ionic strength, and, most importantly, force field. A polymer of PEG, with the number of units  $n$ , is depicted in Figure 1. Unfortunately, the values for  $n$  that can be investigated using MD simulation on sufficiently long time scales to observe convergence is limited due to finite computing power available. Here we use  $n$  values ranging from 2 to 46, *i.e.* low molecular weight PEG. In contrast, experimental studies often involve high molecular weight PEG, *i.e.*  $n \approx 10^3 - 10^4$ .

When comparing experimental data with results obtained from simulation, one

should keep in mind the differences between the simulated and experimentally investigated systems. First, in experimental studies generally much longer PEG chains are present. Second, in the present MD study the chain-terminal groups of the simulated molecules are methoxy-groups (Figure 1), whereas most experimental studies have been carried out with hydroxy-groups as chain-terminal groups. Yet, we have used methoxy terminal groups rather than hydroxy ones, because we wished to keep chain-end influence upon the conformational behaviour of the chain as small as possible. This in view of the relatively short chain lengths that could be simulated with reasonable computing effort and the fact that the hydrogen-bond donor strength of a hydroxyl group is greater than that of a methoxy group.

## 2 Computational Methods

### 2.1 Molecular Dynamics Simulations

MD simulations were performed with the GROMOS software package [25–27] using the GROMOS force-field parameter sets 45A3 [28], 53A6 [29], and 53A6\_OE, which contains a modification of the non-bonded interaction parameters (charges, van der Waals) of the ether oxygen (OE) in the 53A6 force field. The partial charge of the ether oxygen OE was changed from  $-0.32 e$  (53A6) to  $-0.42 e$  (53A6\_OE) and the

partial charges of its adjacent CH<sub>2</sub> united atoms were changed from +0.16 *e* (53A6) to +0.21 *e* (53A6\_OE). The attractive van der Waals parameter (C<sub>6</sub>(OE, OE))<sup>1/2</sup> for the ether oxygen was changed from 0.04756 (kJ mol<sup>-1</sup> nm<sup>6</sup>)<sup>1/2</sup> for the 53A6 parameter set to the value 0.06313 (kJ mol<sup>-1</sup> nm<sup>6</sup>)<sup>1/2</sup> for the 53A6\_OE one. The repulsive van der Waals parameter (C<sub>12</sub>(OE, OE))<sup>1/2</sup> for interactions with non-polar atoms was changed from 1.100×10<sup>-3</sup> (kJ mol<sup>-1</sup> nm<sup>12</sup>)<sup>1/2</sup> for 53A6 to the value 2.148×10<sup>-3</sup> (kJ mol<sup>-1</sup> nm<sup>12</sup>)<sup>1/2</sup> for 53A6\_OE, while the value for interactions with polar atoms remained unmodified at 1.227×10<sup>-3</sup> (kJ mol<sup>-1</sup> nm<sup>12</sup>)<sup>1/2</sup> for both parameter sets and the value for interactions with charged atoms was changed from 1.227×10<sup>-3</sup> (kJ mol<sup>-1</sup> nm<sup>12</sup>)<sup>1/2</sup> for 53A6 to the value of 1.748×10<sup>-3</sup> (kJ mol<sup>-1</sup> nm<sup>12</sup>)<sup>1/2</sup> for 53A6\_OE. In addition, one other, non-GROMOS parameter set has been used, a parameter set by Smith *et al.* [30]. The performed MD simulations are summarized in Table 1.

The initial structure of  $\alpha,\omega$ -dimethoxypolyethylene glycol was chosen to be an elongated conformation modelled using the INSIGHTII software package (Accelrys Inc., San Diego, CA). The simple-point-charge (SPC) water model [31] was used to describe the solvent molecules. In the simulations the solvent molecules were added around the solute within a cubic box with a minimum distance of 1.4 nm between the solute atoms and the walls of the periodic box. In some of the simulations, ions (SO<sub>4</sub><sup>2-</sup> and Ca<sup>2+</sup>) were included. The initial placement of the ions was ran-

dom. All the bonds and the geometry of the water molecules were kept fixed with a geometric tolerance of  $10^{-4}$  using the SHAKE algorithm [32]. A steepest-descent energy minimisation without any restraints of all systems was performed to relax the solute-solvent contacts. The energy minimisations were terminated when the energy change per step became smaller than  $0.1 \text{ kJ mol}^{-1}$ . For the non-bonded interactions, a triple-range method with cutoff radii of 0.8/1.4 nm was used. Short-range van der Waals and electrostatic interactions were evaluated every time step based on a charge-group pairlist. Medium-range van der Waals and electrostatic interactions, between pairs at a distance longer than 0.8 nm and shorter than 1.4 nm, were evaluated every fifth time step, at which time point the pair list was updated. Outside the longer cutoff radius a reaction-field approximation [33] was used with a relative dielectric permittivity of 66 [34]. Newton's equations of motion were integrated using the leap-frog scheme and a time step of 2 fs. The initial velocities of the atoms were assigned from a Maxwell distribution at 50 K. A 10 ps period of MD simulation at constant volume was performed, followed by 100 ps of MD. Solvent and solute were independently, weakly coupled to a temperature bath of the given temperature with a relaxation time of 0.1 ps [35]. In the further simulations, the center of mass motion of the whole system was removed every 1000 time steps. The systems were also weakly coupled to a pressure bath of 1 atm with a relaxation time of 0.5 ps and

an isothermal compressibility of  $0.4575 \times 10^{-3} \text{ (kJ mol}^{-1} \text{ nm}^{-3})^{-1}$ . The trajectory coordinates and energies were saved every 0.5 ps for analysis.

To investigate hydrophobic interactions between and clustering behaviour of the chains, simulations of  $\alpha,\omega$ -dimethoxypolyethylene glycol ( $n = 23$ ) with every third unit methoxylated (see label "ome" in Table 1) and simulations of  $\alpha,\omega$ -dimethoxypolyethylene glycol ( $n = 46$ ) cut into several pieces (see label "cut" or "cuts" in Table 1) were also performed. For the latter the final configurations of the uncut chain simulations were used as starting configurations, followed by one more round of energy minimisation and MD equilibration following the above mentioned procedure. For polyethylene glycol the same starting structures were used for simulations with the terminal methoxy-groups substituted by hydroxyl-groups.

The free enthalpy of solvation was calculated using thermodynamic integration (TI) [36]. To remove  $\alpha,\omega$ -dimethoxypolyethylene glycol from the system all non-bonded interactions involving solute atoms were scaled down to zero in a stepwise manner as a function of the coupling parameter  $\lambda$ . The free-enthalpy change corresponding to the removal of all solute non-bonded interactions was then calculated by integrating the average value of the derivative of the Hamiltonian of the system with respect to  $\lambda$ . This integral was evaluated using 21 evenly spaced  $\lambda$ -values with 30 ps of equilibration and 160 ps of data collection at each  $\lambda$ -value. Soft-core interaction



was used in order to avoid singularities in the non-bonded interaction function at particular  $\lambda$ -values [37]. The free enthalpy of solvation was then calculated as the difference between the free enthalpy change of letting the solute disappear in vacuo and the free enthalpy change of letting the solute disappear in solution.

## 2.2 Analysis

Analyses were done with the analysis software packages GROMOS++ [27] and esra [38]. Radii of gyration were calculated with respect to a given set of atoms to observe the level of compactness of the simulated solute molecules. Structural information on solutions was obtained from atom-atom radial distribution functions,  $g(r)$ . Percentages of intermolecular hydrogen bonds have been calculated using a maximum distance criterion of 0.25 nm between the hydrogen atom and the acceptor atom, and a minimum angle criterion of  $135^\circ$  for the donor-hydrogen-acceptor angle. In order to further investigate the compaction properties of the  $\alpha,\omega$ -dimethoxypolyethylene glycol chains solute oxygen-oxygen distance distributions  $d(O_i-O_j)$  and percentages of water molecules bridging between solute oxygen atoms were calculated. The bridging waters have been determined using a maximum distance criterion of 0.75 nm between two bridged solute-oxygen atoms and a maximum distance criterion of 0.36 nm between the solute-oxygen atoms and the bridging-water oxygen atom.

### 3 Results

In Figure 2 the radii of gyration for  $\alpha,\omega$ -dimethoxypolyethylene glycol ( $n = 9, 11, 15, 23, 46$ ) are presented for the simulations `peg_no_ions_n` ( $n = 9, 11, 15, 23, 46$ ) and different force fields. For the GROMOS 53A6 force field the radii of gyration of the chains of different lengths converge to values between 0.50 and 0.75 nm. This indicates a compaction of the chains, keeping in mind that the initial structures were chosen to be elongated. At 313 K the compact state is reached faster than at low temperature due to faster sampling at higher temperatures. The simulations of  $\alpha,\omega$ -dimethoxypolyethylene glycol with the force field 53A6\_OE and that of Smith *et al.* show larger, more fluctuating radii of gyration, suggesting that here the chains remain elongated and do not form compact conformations.

The radii of gyration for a chain of length  $n = 23$  in Figure 3 show again the compacting behaviour of  $\alpha,\omega$ -dimethoxypolyethylene glycol in water this time for the GROMOS 45A3 force field. The GROMOS force fields 53A6 (Figure 2) and 45A3 (Figure 3) show similar behaviour, they reach the same radius of gyration, and converge to a stable value equally quickly. When adding  $\text{Ca}^{2+}$  and  $\text{SO}_4^{2-}$  ions to the solution,  $\alpha,\omega$ -dimethoxypolyethylene glycol also forms compact structures, the radii of gyration being similar to those of the simulations in pure water (Figure 3,  $\text{CaSO}_4$ ). The methoxylated solute shows behaviour similar to that of the unmethoxylated one

(Figure 3, ome). In the solvents methanol, carbon tetrachloride, and dimethylsulfoxide the polymer does not show the compacting behaviour observed in water (Figure 3, CCl<sub>4</sub>, DMSO). The radii of gyration do fluctuate much more than in water and around a value that is twice as large as the one in water. The force fields 53A6\_OE and that by Smith *et al.* [30] perform differently from the GROMOS 45A3 and 53A6 force fields in water, but behave similarly in methanol. For the simulations in methanol the polymer seems to be elongated in all cases.

In Figure 4 the radial distribution functions,  $g(r)$ , between different atom pairs are shown for the GROMOS force field 53A6 and the force field by Smith *et al.* [30]. The solute oxygen atoms (OE) show no coordination with calcium (Ca) or sulfate ions (SO<sub>4</sub>) in any of the simulations, so their  $g(r)$ 's are not shown. The  $g(r)$  of calcium and sulfate in Figure 4A shows interesting behaviour: at higher temperature there is higher coordination of sulfate to calcium in the first two solvation shells. This indicates entropically favoured clustering of these ions. All other radial distribution functions have similar shapes at the two different temperatures. Calcium and sulfate are solvated by water (OW), the first solvation shell of calcium being more structured (Figures 4B and 4C). The coordination of solute oxygen atoms (OE) with water oxygen atoms is not significant. This is the case for the GROMOS force fields as well as for the force field by Smith *et al.* [30]. The Smith force field shows slightly

more structured solute oxygen solvation in the first solvation shell at 278 K.

The results of the hydrogen-bond and bridging-water analyses do not bring forward any significant percentage of water molecules that stay coordinated between different solute-oxygen atoms (Results not shown).

In Figure 5, solute oxygen-oxygen distance distributions  $d(O_i-O_j)$  are shown for the simulations of  $\alpha,\omega$ -dimethoxypolyethylene glycol. Distance distributions have been calculated for oxygen atoms belonging to units  $i$  and  $j$  that have a given distance  $n = |i - j| \geq 2$  along the chain from each other. Especially for the oxygen atoms that are further away along the chain the difference between the simulations in water and those in methanol becomes striking. Larger distances have a larger probability to occur in methanol, illustrating the non-compact conformations of the polymer in methanol. The illustrations confirm the suggestion that with the force field 53A6\_OE and that of Smith *et al.* [30] the structure is more elongated, showing wider distributed end-to-end lengths.

The tendency for compaction of the polyethylene glycol chains when simulated using the 53A6 force field was investigated by cutting the larger chains into smaller segments and observing the relative motion of the latter as expressed by the radius of gyration of the cluster of segments. The radii of gyration calculated from the 53A6 simulations of an  $\alpha,\omega$ -dimethoxypolyethylene glycol ( $n = 46$ ) molecule cut into

pieces of different sizes are shown in Figure 6. The radius of gyration calculated over all atoms reaches a value of about 0.75 nm in the case of 1, 3 and 8 cuts for  $\alpha,\omega$ -dimethoxypolyethylene glycol, a value very similar to the value obtained from the simulations of the intact chain.  $\alpha,\omega$ -dimethoxypolyethylene glycol cut into 16 pieces shows diffusive behaviour at 313 K after 2.5 ns. The simulations of polyethylene glycol behave similarly in the case of 8 cuts, only when going to smaller chain lengths (15 cuts) the solutes show diffusive behaviour, even at 278 K. After 1 ns of simulation the cluster members start to move away from each other. Of course it is possible to extend the simulations beyond 3 ns to test whether larger segments will dissociate on longer time scales, but because the 53A6 force field shows too much compaction, a further investigation of those properties does not seem warranted. Because the 53A6\_OE and Smith force fields show no compaction for single chains, an investigation of clustering of smaller segments makes no sense.

In Table 2 free enthalpies of solvation for chains of two different sizes of  $\alpha,\omega$ -dimethoxypolyethylene glycol ( $n = 6$ ) are listed. Free enthalpies have been calculated using the force fields 53A6 and 53A6\_OE in the solvents water and methanol. Using force field 53A6  $\alpha,\omega$ -dimethoxypolyethylene glycol is better solvated in methanol than in water, whereas using 53A6\_OE force field it is better solvated in water than in methanol. The too small free enthalpy of hydration found for the 53A6 force field

may explain the compaction of the PEG chains observed in the 53A6 simulations in water.

## 4 Discussion

In the present work  $\alpha,\omega$ -dimethoxypolyethylene glycol of different chain lengths and composition has been simulated under various conditions: different force fields, temperatures, and solvents.

The GROMOS force fields 45A3 and 53A6 induce similar behaviour, giving  $\alpha,\omega$ -dimethoxypolyethylene glycol a rather hydrophobic character, forming compact structures when simulated in water. The compact structures are not formed due to water molecules bridging between the solute oxygen atoms of different ethylene oxide units as is concluded from bridging water analyses. The helical structure found in the molecular dynamics study by Tasaki [20] was not observed here. This difference may be due to the different type of force and simulation set-up used in [20]. An indication of the hydrophobic behaviour of  $\alpha,\omega$ -dimethoxypolyethylene glycol using the 45A3 and 53A6 force fields is that in less polar solvents, such as methanol, DMSO, and carbon tetrachloride, the molecule does not form a compact aggregate. This observation is confirmed by the solute-oxygen-oxygen distance distribution analysis:  $\alpha,\omega$ -dimethoxypolyethylene glycol's solute oxygen atoms tend to separate further

from each other in solvents that are less polar than water. Free enthalpies of solvation show that different oligomers of  $\alpha,\omega$ -dimethoxypolyethylene glycol are dissolved better in methanol than in water using the 53A6 force field. When simulating clusters of  $\alpha,\omega$ -dimethoxypolyethylene glycol molecules of different number and size of the molecules, the molecules tend to stay aggregated except for very short chains and very small clusters. When simulating clusters of  $\alpha,\omega$ -dimethoxypolyethylene glycol trimers and dimers the clusters fall apart. The interaction of  $\alpha,\omega$ -dimethoxypolyethylene glycol with calcium and sulfate ions is not significant at all, the ions rather interact with each other than with PEG's oxygen atoms.

The behaviour of the simulated PEG chains as observed for the GROMOS 45A3 and 53A6 force fields seems different from the behaviour documented from experiment in the literature. We find compact structures for molecules that are observed [10, 11] to be well soluble in water. Light scattering of high molecular weight PEG suggests that PEG is less extended in methanol than in water [10, 11], which is the opposite of what was found in the present study of low molecular weight PEG. Another discrepancy between simulation and experiment is that the simulated short PEG chains show tendencies to form clusters, whereas an experimental study suggested that PEG chains forcibly moved towards each other show repulsive interactions [18, 19]. These discrepancies between simulation and experiment are re-

solved when using the GROMOS 53A6\_OE force field or the one by Smith *et al.* [30]. They produce markedly different results from the GROMOS 45A3 and 53A6 force fields. Using the former, the PEG chains prefer elongated conformations, in water as well as in methanol, thus reproducing experimentally observed data more accurately. The different simulation results, compaction, aggregation, and free enthalpies of solvation, offer a consistent picture of short-chain PEG conformational properties in solution. The GROMOS 53A6\_OE parameter set is a clear improvement over the 53A6 one. We note that the parameters of the GROMOS 53A6 force field used were optimised to reproduce thermodynamic properties of a series of small non-polar and polar compounds representing segments of biomolecules [28,29]. Their solvation free energies in a variety of solvents, such as the ones used here, do match very well their experimental counterparts [39]. However, the calibration set of small compounds did not comprise ether moieties, which may explain the poor behaviour of the 53A6 parameter set for PEG. The results of our comparison of four force fields for PEG illustrate the importance of using an appropriate force field in molecular simulation to understand structural behaviour of flexible molecules.



## 5 Acknowledgements

Financial support was obtained from the National Center of Competence in Research (NCCR) in Structural Biology and from grant number 200021-109227 of the Swiss National Science Foundation, which is gratefully acknowledged. Moritz Winger acknowledges Daan Geerke for fruitful and inspiring discussions.

## References

- [1] A. Abuchowski, G.M. Kazo, C.R. Verhoest *et al.*, Cancer therapy with chemically modified enzymes. I. Antitumor properties of polyethylene glycol-asparaginase conjugates *Cancer Biochem. Biophys.* **7**, 175–186 (1984).
- [2] P.A. Albertsson, *Partiton of Cell Particles and Macromolecules* 1986.
- [3] M.S. Hershfield, R.H. Buckley, M.L. Greenburg *et al.*, Treatment of adenosine deaminase deficiency with polyethylene glycol-modified adenosine deaminase *New Eng. J. Med.* **316**, 589–596 (1987).
- [4] J.S. Beckmann, R.L. Minor, C.W. White *et al.*, Superoxide dismutase and catalase conjgated to polyethylene glycol increases endothelial enzyme activity and oxidant resistance *J. Biol. Chem.* **263**, 6884–6892 (1988).
- [5] Y. Inada, A. Matsushima, Y. Kodera and H. Nishimura, Alteration of properties of natural pigments by conjugation with fibroin or polyethylene glycol *J. Bioact. Compat. Polym.* **5**, 343–364 (1990).
- [6] J.M. Harris, editor, *Poly(Ethylene Glycol) Chemistry* 1992.
- [7] P. Molyneux, editor, *Water-soluble Synthetic Polymers: Properties and Uses* 1983.

- [8] E.E. Bailey Jr. and J.V. Koleske, editors, *Alkylene Oxides and Their Polymers: Surfactant Science Series* 1991.
- [9] E.E. Bailey Jr. and J.V. Koleske, *Poly (ethylene oxide)* 1976.
- [10] K. Devanand and J.C. Selser, Asymptotic behaviour and long-range interactions in Aqueous solutions of Poly(ethylene oxide) *Macromolecules* **24**, 5943–5947 (1991).
- [11] K. Devanand, Polyethylene oxide does not necessarily aggregate in water *Nature* **343**, 739–741 (1990).
- [12] S. Kawaguchi, G. Imai, J. Suzuki *et al.*, Aqueous solution properties of oligo- and poly(ethylene oxide) by static light scattering and intrinsic viscosity *Polymer* **38**, 2885–2891 (1997).
- [13] K. Tasaki and A. Abe, NMR studies and conformational energy calculations of 1,2-Dimethoxyethane and Poly(oxyethylene) *Polym. J.* **17**, 641–655 (1985).
- [14] J.L. Koenig and A.C. Angood, Raman spectra of poly(ethylene glycols) in solution *J. Polym. Sci.* **8**, 1787–1796 (1970).
- [15] K.J. Liu and J.L. Parsons, Chain flattening and infrared dichroism of adsorbed poly(ethylene oxide) *Macromolecules* **2**, 529–533 (1969).

- [16] H. Matsuura and K.J. Fukuhara, Conformational behaviour of short poly(oxyethylene) compounds in formamide: a Raman spectroscopic study *J. Mol. Struct.* **126**, 251–260 (1985).
- [17] J. Maxfield and I.W. Shepherd, Polyethylene oxide does not necessarily aggregate in water *Polymer* **16**, 505–509 (1975).
- [18] U. Raviv, J. Frey, R. Sak *et al.*, Properties and Interactions of Physigrafted End-Functionalized Poly(ethylene glycol) Layers *Langmuir* **18**, 7482–7495 (2002).
- [19] T. Drobek, N.D. Spencer and M. Heuberger, Compressing PEG Brushes *Macromolecules* **38**, 5254–5259 (2005).
- [20] K. Tasaki, Poly(oxyethylene)-water interactions: A molecular dynamics study *J. Am. Chem. Soc.* **118**, 8459–8469 (1996).
- [21] G.D. Smith and D. Bedrov, A molecular dynamics simulation study of the influence of hydrogen-bonding and polar interactions on hydration and conformations of a poly(ethylene oxide) oligomer in dilute aqueous solution *Macromolecules* **35**, 5712–5719 (2002).
- [22] O. Borodin, F. Trouw, D. Bedrov and G.D. Smith, Temperature Dependence of Water Dynamics in Poly(Ethylene Oxide)/Water Solutions from Molecu-

- lar Dynamics Simulations and Quasielastic Neutron Scattering Experiments J. Phys.Chem. B **106**, 5184–5193 (2002).
- [23] M. Polverari and T.G.M. van de Ven, Association-induced polymer bridging by poly(ethylene oxide)cofactor flocculation systems J. Phys. Chem. **100**, 13687–13695 (1996).
- [24] R. Kjellander and E. Florin, Water Structure and Changes in Thermal Stability of the System Poly(ethylene oxide)-Water J. Chem. Soc. Faraday Trans. **77**, 2053–2077 (1981).
- [25] W.F. van Gunsteren, S.R. Billeter, A.A. Eising *et al.*, *Biomolecular simulation: The GROMOS96 manual and user guide*. 1996.
- [26] W.R.P. Scott, P.H. Hünenberger, I.G. Tironi *et al.*, The GROMOS Biomolecular Simulation Program Package J. Phys. Chem. A. **103**, 3596–3607 (1999).
- [27] M. Christen, P. Hünenberger, D. Bakowies *et al.*, The GROMOS software for biomolecular simulation: GROMOS05 J. Comput. Chem. **26**, 1719–1751 (2005).
- [28] L. Schuler, X. Daura and W. van Gunsteren, An Improved GROMOS96 Force Field for Aliphatic Hydrocarbons in the Condensed Phase J. Comp. Chem. **22**, 1205–1218 (2001).

- [29] C. Oostenbrink, A. Villa, A.E. Mark and W.F. van Gunsteren, A biomolecular force field based on the free enthalpy of hydration and solvation: The GROMOS force-field parameter sets 53A5 and 53A6 J. Comput. Chem. **25**, 1656–1676 (2004).
- [30] D. Bedrov, M. Pekny and D.G. Smith, Quantum-Chemistry-Based Force Field for 1,2-Dimethoxyethane and Poly(ethylene oxide) in Aqueous Solution J. Phys. Chem. B **102**, 996–1001 (1998).
- [31] H.J.C. Berendsen, J.P.M. Postma, W.F. van Gunsteren and J. Hermans, Interaction models for water in relation to protein hydration, in *Intermolecular Forces*, edited by B. Pullman (Reidel, Dordrecht, 1981), pp. 331–342.
- [32] J.P. Ryckaert, G. Ciccotti and H.J.C. Berendsen, Numerical Integration of the Cartesian Equations of Motion of a System with Constraints: Molecular Dynamics of n-Alkanes J. Comput. Phys. **23**, 327–341 (1977).
- [33] I.G. Tironi, R. Sperb, P.E. Smith and W.F. van Gunsteren, A generalized reaction field method for molecular dynamics simulations J. Chem. Phys. **102**, 5451–5459 (1995).
- [34] A. Glättli, X. Daura and W.F. van Gunsteren, Derivation of an improved simple point charge model for liquid water: SPC/A and SPC/L J. Chem. Phys. **116**,

9811–9828 (2002).

- [35] H.J.C. Berendsen, J.P.M. Postma, W.F. van Gunsteren *et al.*, Molecular dynamics with coupling to an external bath *J. Chem. Phys.* **81**, 3684–3690 (1984).
- [36] D.L. Beveridge and F.M. DiCapua, Free energy via molecular simulation: applications to chemical and biomolecular systems *Annu. Rev. Biophys. Biophys. Chem.* **18**, 431–492 (1989).
- [37] T.C. Beutler, A.E. Mark, R.C. van Schaik *et al.*, Avoiding singularities and numerical instabilities in free energy calculations based on molecular simulations *Chem. Phys. Lett.* **222**, 529–539 (1994).
- [38] V. Kräutler, M. Kastenholz and P.H. Hünenberger, The esra molecular mechanics analysis package available at <http://esra.sf.net/> (2005).
- [39] D.P. Geerke and W.F. van Gunsteren, Force Field Evaluation for Biomolecular Simulation: Free Enthalpies of Solvation of Polar and Apolar Compounds in Various Solvents *ChemPhysChem* **7**, 671–678 (2006).

## Table captions

Table 1 : Overview of the performed MD simulations on  $\alpha,\omega$ -dimethoxypolyethylene glycol (polyethylene glycol, PEG). The label "ome" indicates PEG with every third unit methoxylated. The label "oh" indicates PEG with hydroxy-groups at the chain termini. The labels "cut" or "cuts" indicate that the PEG chain is cut into a given number of separate pieces.

Table 2 : Free enthalpies of solvation of  $\alpha,\omega$ -dimethoxypolyethylene glycol ( $n = 6$ ) calculated using the GROMOS force fields 53A6 and 53A6\_OE in water and methanol at 278 K and 1 atm.



Table 1:

simulation label	chain length	number of counterions	end groups	force-field parameter set	solvent	simulation length / ns
peg_no_ions_46_53A6	46	0	OCH <sub>3</sub>	53A6	H <sub>2</sub> O	5
peg_no_ions_46_53A6_OE	46	0	OCH <sub>3</sub>	53A6_OE	H <sub>2</sub> O	5
peg_no_ions_46_Smith	46	0	OCH <sub>3</sub>	Smith	H <sub>2</sub> O	4.5
peg_no_ions_23_45A3	23	0	OCH <sub>3</sub>	45A3	H <sub>2</sub> O	4.8
peg_no_ions_23_53A6	23	0	OCH <sub>3</sub>	53A6	H <sub>2</sub> O	4.5
peg_no_ions_23_53A6_OE	23	0	OCH <sub>3</sub>	53A6_OE	H <sub>2</sub> O	5
peg_no_ions_23_Smith	23	0	OCH <sub>3</sub>	Smith	H <sub>2</sub> O	5
peg_no_ions_23_53A6_meoh	23	0	OCH <sub>3</sub>	53A6	CH <sub>3</sub> OH	4
peg_no_ions_23_53A6_OE_meoh	23	0	OCH <sub>3</sub>	53A6_OE	CH <sub>3</sub> OH	5
peg_no_ions_23_Smith_meoh	23	0	OCH <sub>3</sub>	Smith	CH <sub>3</sub> OH	5
peg_no_ions_23_53A6_dmsol	23	0	OCH <sub>3</sub>	53A6	DMSO	4.4
peg_no_ions_23_53A6_ccl4	23	0	OCH <sub>3</sub>	53A6	CCl <sub>4</sub>	2.6
peg_no_ions_15_53A6	15	0	OCH <sub>3</sub>	53A6	H <sub>2</sub> O	3.5
peg_no_ions_15_53A6_OE	15	0	OCH <sub>3</sub>	53A6_OE	H <sub>2</sub> O	3.7
peg_no_ions_15_Smith	15	0	OCH <sub>3</sub>	Smith	H <sub>2</sub> O	3.5
peg_no_ions_11_53A6	11	0	OCH <sub>3</sub>	53A6	H <sub>2</sub> O	5
peg_no_ions_11_53A6_OE	11	0	OCH <sub>3</sub>	53A6_OE	H <sub>2</sub> O	3.5
peg_no_ions_11_Smith	11	0	OCH <sub>3</sub>	Smith	H <sub>2</sub> O	3
peg_no_ions_9_53A6	9	0	OCH <sub>3</sub>	53A6	H <sub>2</sub> O	4.5
peg_no_ions_9_53A6_OE	9	0	OCH <sub>3</sub>	53A6_OE	H <sub>2</sub> O	3.5
peg_no_ions_9_Smith	9	0	OCH <sub>3</sub>	Smith	H <sub>2</sub> O	3.2
peg_ome_no_ions_23_53A6	23	0	OCH <sub>3</sub>	53A6	H <sub>2</sub> O	2.4
peg_caso_23_53A6	23	45 Ca <sup>2+</sup> , 45 SO <sub>4</sub> <sup>2-</sup>	OCH <sub>3</sub>	53A6	H <sub>2</sub> O	4.2
peg_caso_23_53A6_OE	23	45 Ca <sup>2+</sup> , 45 SO <sub>4</sub> <sup>2-</sup>	OCH <sub>3</sub>	53A6_OE	H <sub>2</sub> O	3
peg_caso_23_Smith	23	45 Ca <sup>2+</sup> , 45 SO <sub>4</sub> <sup>2-</sup>	OCH <sub>3</sub>	Smith	H <sub>2</sub> O	3.4
peg_no_ions_46_1cut_53A6	2 × 23	0	OCH <sub>3</sub>	53A6	H <sub>2</sub> O	2
peg_no_ions_46_1cut_53A6_OE	2 × 23	0	OCH <sub>3</sub>	53A6_OE	H <sub>2</sub> O	3
peg_no_ions_46_1cut_Smith	2 × 23	0	OCH <sub>3</sub>	Smith	H <sub>2</sub> O	3
peg_no_ions_46_3cuts_53A6	2 × 12 and 2 × 11	0	OCH <sub>3</sub>	53A6	H <sub>2</sub> O	2
peg_no_ions_46_8cuts_53A6	5 × 5 and 1 × 6	0	OCH <sub>3</sub>	53A6	H <sub>2</sub> O	3
peg_no_ions_46_8cuts_Smith	5 × 5 and 1 × 6	0	OCH <sub>3</sub>	Smith	H <sub>2</sub> O	3
peg_no_ions_46_15cuts_53A6	14 × 3 and 2 × 2	0	OCH <sub>3</sub>	53A6	H <sub>2</sub> O	2
peg_oh_no_ions_46_8cuts_53A6	5 × 5 and 1 × 6	0	OH	53A6	H <sub>2</sub> O	2
peg_oh_no_ions_46_15cuts_53A6	14 × 3 and 2 × 2	0	OH	53A6	H <sub>2</sub> O	2
peg_no_ions_6_free.energy_h2o_53A6	6	0	OCH <sub>3</sub>	53A6	H <sub>2</sub> O	21 × (0.03 + 0.16)
peg_no_ions_6_free.energy_meoh_53A6	6	0	OCH <sub>3</sub>	53A6	CH <sub>3</sub> OH	21 × (0.03 + 0.16)

peg_no_ions_6_free_energy_h2o_53A6_OE	6	0	OCH <sub>3</sub>	53A6_OE	H <sub>2</sub> O	21 × (0.03 + 0.16)
peg_no_ions_6_free_energy_meoh_53A6_OE	6	0	OCH <sub>3</sub>	53A6_OE	CH <sub>3</sub> OH	21 × (0.03 + 0.16)

---

Table 2:

system	force field	$\Delta G_{solv,water}$ [kJ/mol]	$\Delta G_{solv,ethanol}$ [kJ/mol]
$\alpha,\omega$ -dimethoxypolyethylene glycol (n = 6)	53A6	-5.6	-43.7
$\alpha,\omega$ -dimethoxypolyethylene glycol (n = 6)	53A6_OE	-86.12	-86.03

## Figure captions

Figure 1 : Simulated polymers:  $\alpha,\omega$ -dimethoxypolyethylene glycol (PEG),  $\alpha,\omega$ -dimethoxypolyethylene glycol methoxylated every third residue (PEG\_ome), polyethylene glycol (PEG\_oh). n indicates the number of repeating units.

Figure 2 : Radii of gyration of chains of different lengths (n) of  $\alpha,\omega$ -dimethoxypolyethylene glycol simulated in water with the force field 53A6 at 278 K (black) and 313 K (red) and with the force field 53A6\_OE (blue) and that of Smith *et al.* [30] (green), each at 278 K, as function of simulation time (Simulations peg\_no\_ions\_n\_53A6, peg\_no\_ions\_n\_53A6\_OE, peg\_no\_ions\_n\_Smith, with n = 46, 23, 15, 11, and 9, see Table 1).

Figure 3 : Radii of gyration of  $\alpha,\omega$ -dimethoxypolyethylene glycol (n = 23) for force field 45A3 and for various solute and solvent compositions at 278 K: black: peg\_no\_ions\_23\_45A3, red: peg\_ome\_no\_ions\_23\_53A6, green: peg\_no\_ions\_23\_53A6\_dms, blue: peg\_no\_ions\_23\_53A6\_ccl4, yellow: peg\_no\_ions\_23\_53A6\_meoh, brown: peg\_no\_ions\_23\_Smith\_meoh, grey: peg\_no\_ions\_23\_53A6\_OE\_meoh, purple: peg\_caso\_23\_53A6, turquoise: peg\_caso\_23\_Smith.

Figure 4 : Radial distribution functions  $g(r)$  for the simulation of  $\alpha,\omega$ -dimethoxypolyethylene glycol (n = 23) in calcium sulfate solutions: black: peg\_caso\_23\_53A6

at 278 K, red: peg\_caso\_23\_53A6 at 313 K, green: peg\_caso\_23\_53A6\_OE at 278 K. The four plots show the  $g(r)$  between calcium and sulfate oxygen atoms (A), calcium and water oxygen (OW) atoms (B), sulfate and water oxygen atoms (C), and water oxygen atoms and solute oxygen (OE) atoms (D).

Figure 5 : Distance distributions  $d(O_i-O_{i+n})$  for different separations ( $n = 2$  (A),  $n = 4$  (B),  $n = 8$  (C),  $n = 12$  (D),  $n = 18$  (E),  $n = 20$  (F)) of solute oxygen atoms along the solute chain for solvation in water and in methanol at 278 K and 313 K. Simulations: black: peg\_no\_ions\_23\_53A6, red: peg\_no\_ions\_23\_53A6\_meoh, blue: peg\_no\_ions\_23\_OE, green: peg\_no\_ions\_23\_Smith. Solid lines: 278 K, dashed lines 313 K.

Figure 6 : Radii of gyration for the simulations of  $\alpha,\omega$ -dimethoxypolyethylene glycol ( $n = 46$ ) (peg\_no\_ions\_46\_53A6) and polyethylene glycol cut into 2, 4, 9, and 16 pieces (peg\_no\_ions\_46\_1cut\_53A6, peg\_no\_ions\_46\_3cuts\_53A6, peg\_no\_ions\_46\_8cuts\_53A6, peg\_no\_ions\_46\_15cuts\_53A6, peg\_oh\_no\_ions\_46\_8cuts\_53A6, peg\_oh\_no\_ions\_46\_15cuts\_53A6) at 278 K and 313 K.

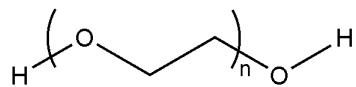
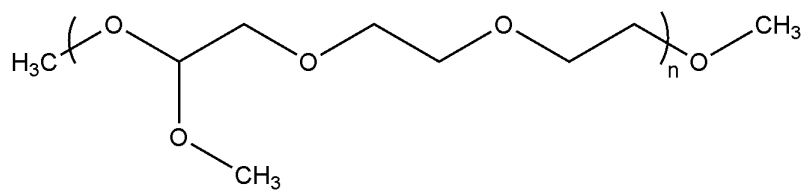
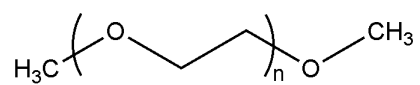


Figure 1:

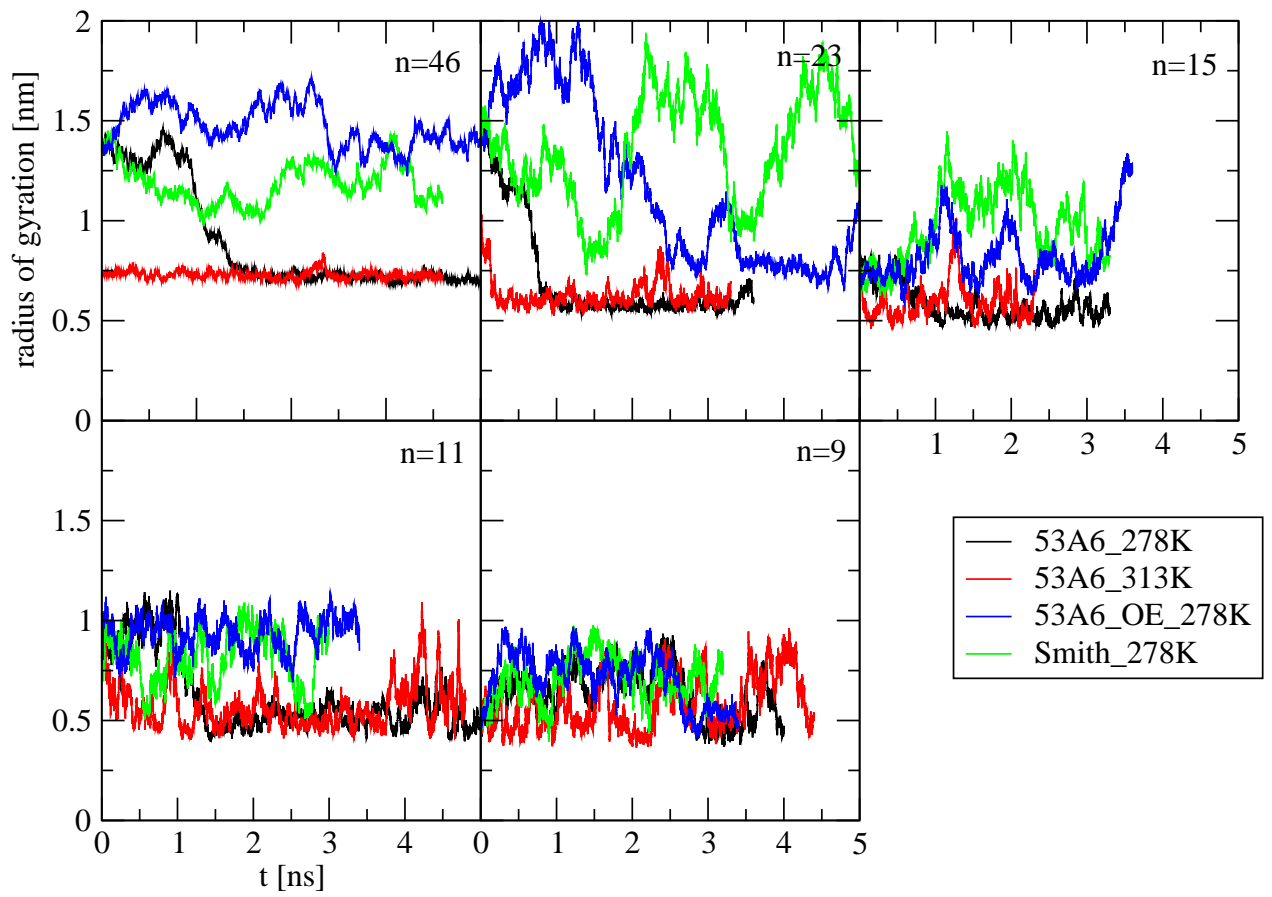


Figure 2:

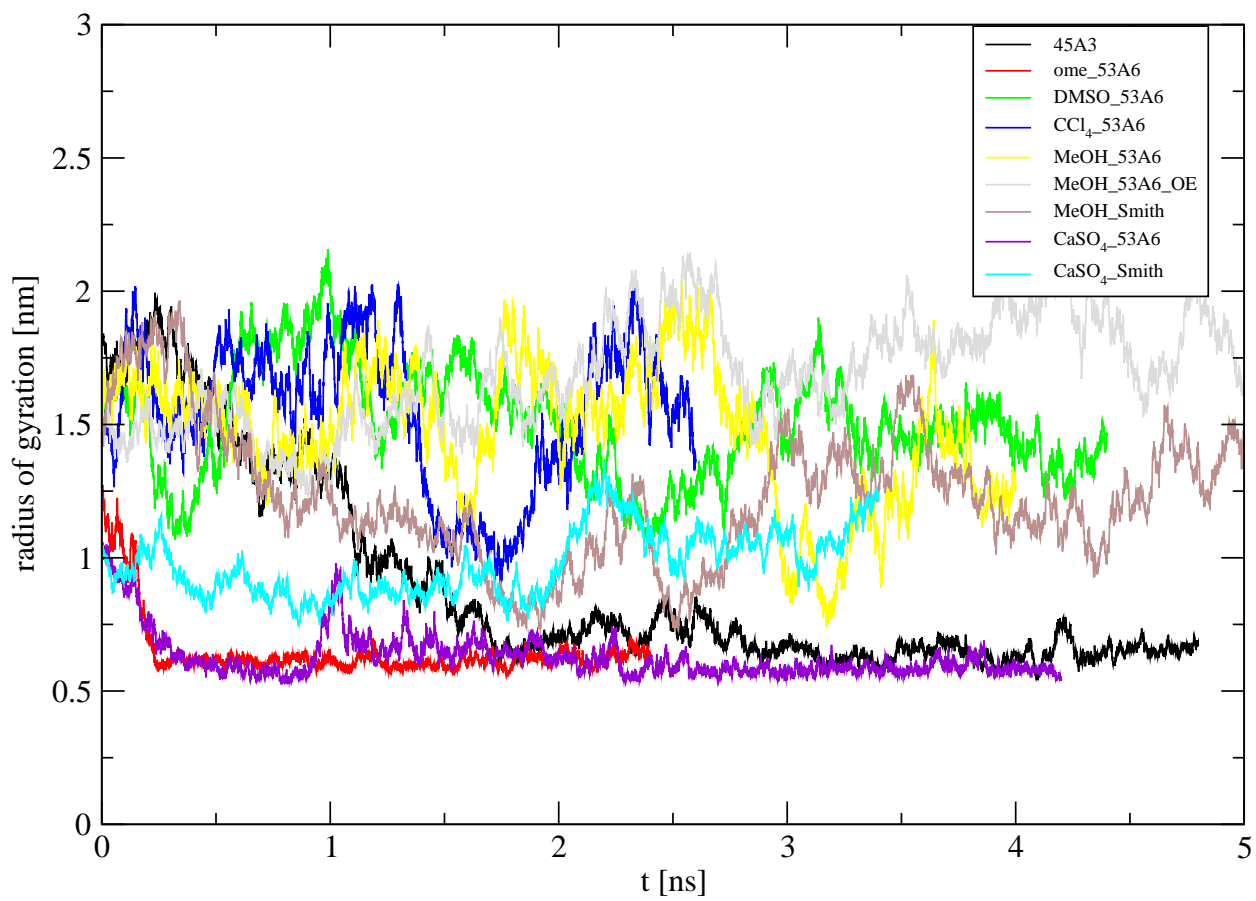


Figure 3:



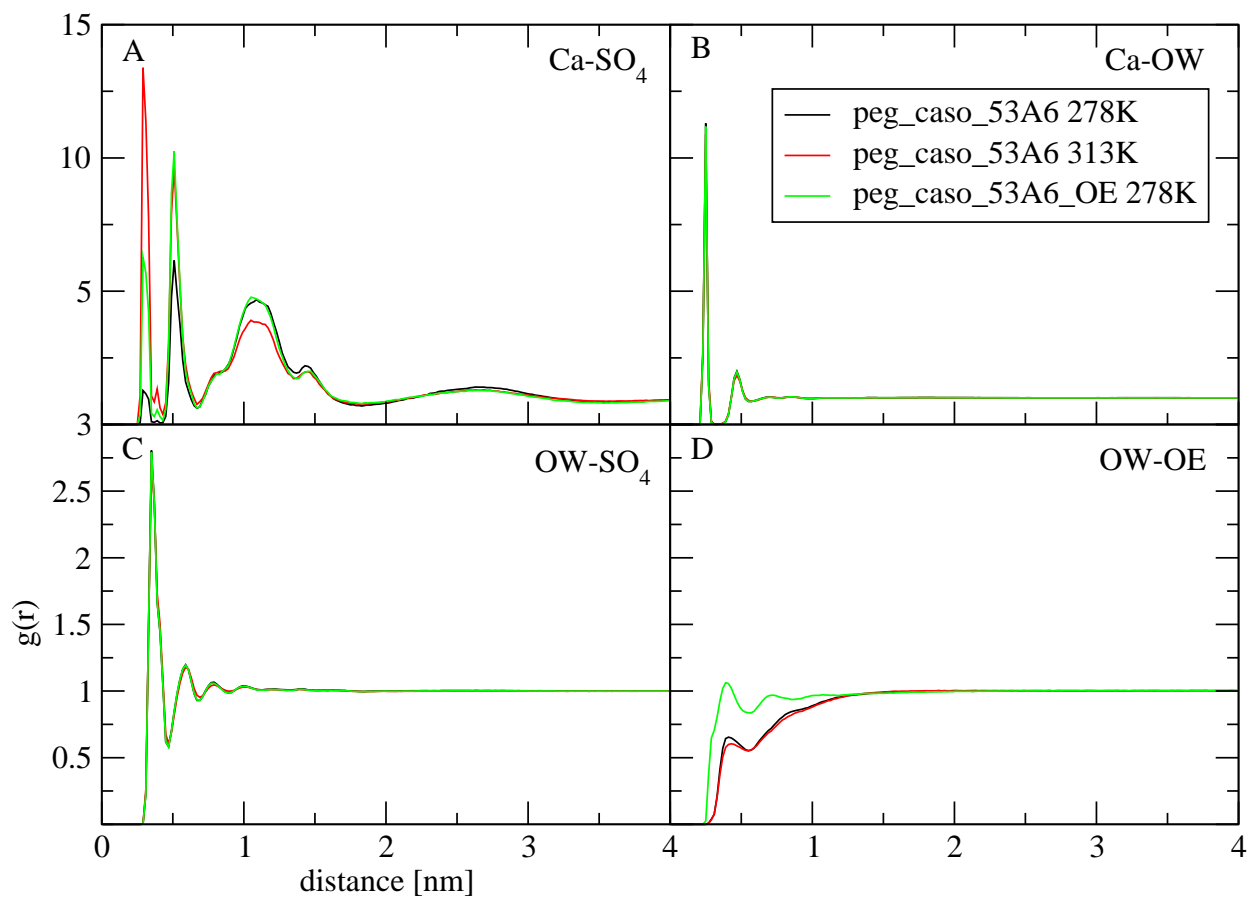


Figure 4:

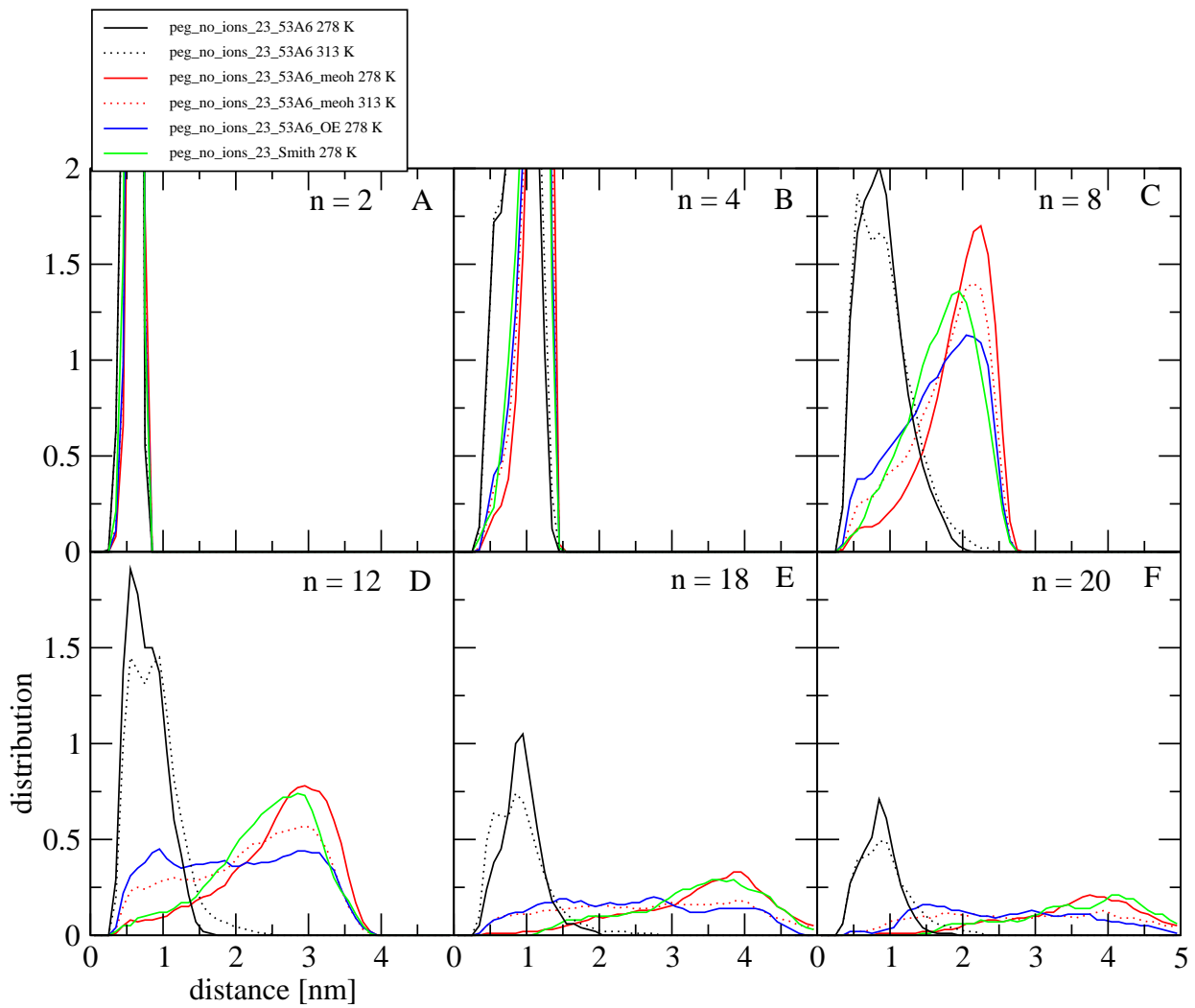


Figure 5:

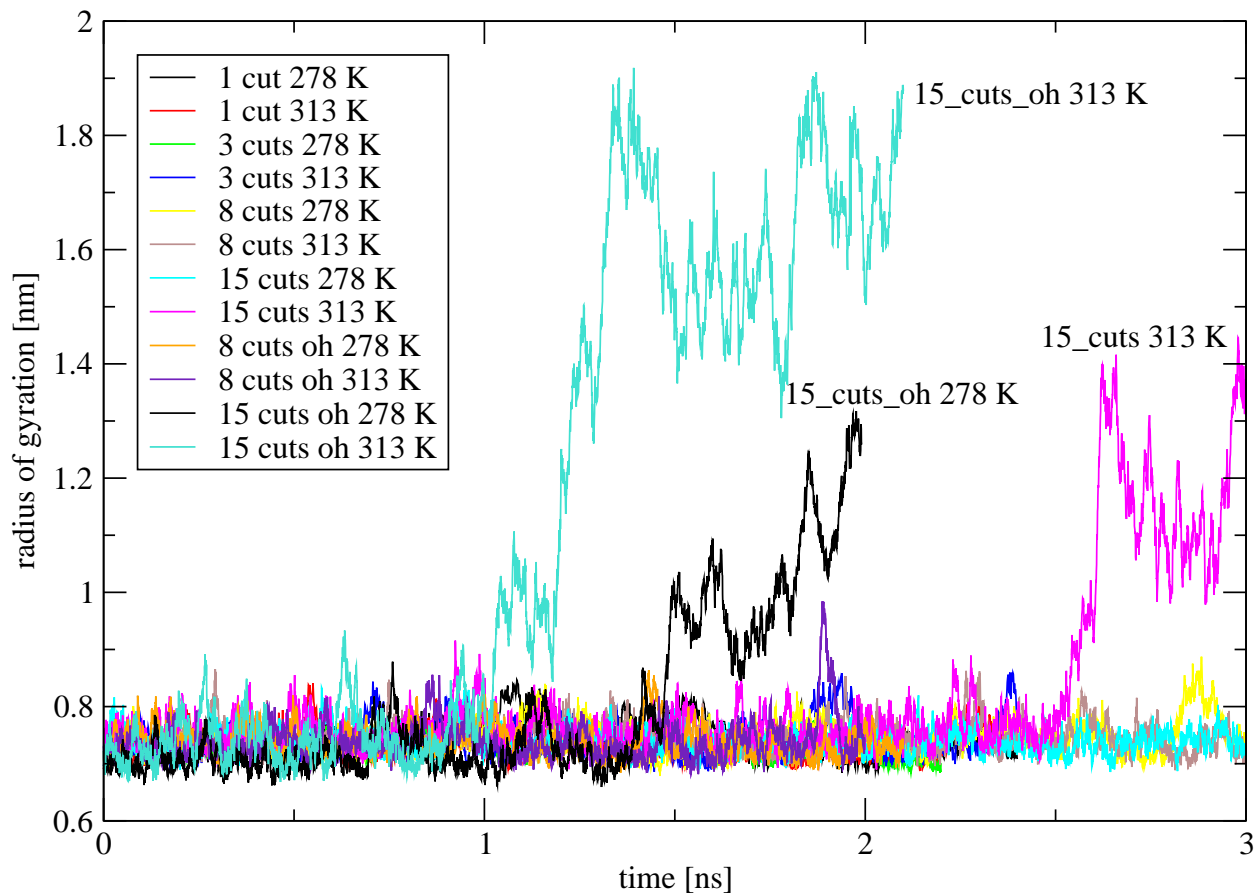


Figure 6: